High-rate low-temperature PVD of thick 10 μm α-alumina coatings

High-rate low-temperature PVD of thick 10 μm α-alumina coatings

N V Gavrilov[1], A S Kamenetskikh[1,2], P V Tretnikov[1] and A V Chukin[2]

[1] Institute of Electrophysics UD RAS, 106 Amundsen Str., Yekaterinburg, 620016, Russia
[2] Ural Federal University, 19 Mira Str., Yekaterinburg, 620002, Russia

E-mail: alx@iep.uran.ru

Abstract. α-Al_2O_3 coatings have been deposited by evaporation of Al in an anodic arc with a growth rate of ~ 5 μm·h^{-1} at 640°C under the conditions of low ionization of the Al vapors and an increased concentration of atomic oxygen, which has been achieved by the use of a hollow anode.Intensive (current density up to 15 mA·cm^{-2}) low-energy (50 eV) ion bombardment has provided deposition of adhesive single-phase nanocrystalline (50–150 nm) α-Al_2O_3 coatings with a thickness of up to 10 μm with low intrinsic stresses (1.5 GPa) and low microstrains of the crystal lattice (less than 0.1%). The composition of the discharge plasma has been determined using the optical spectroscopy method. The effect of the O_2 flow and the hollow anode current on the growth rate of the alumina coatings has been investigated and it has been shown that the increasing degree of O_2 dissociation promotes an increase in the growth rate of coatings.

1. Introduction

High-rate synthesis of thick α-aluminium oxide (α-Al_2O_3) coatings using reactive PVD methods at low temperatures requires solving a number of tasks related to the creation of conditions for the nucleation of the α-phase on the substrate and subsequent rapid growth of α-Al_2O_3 coating with a dense and fairly homogeneous microstructure and low levels of intrinsic stresses that provide a firm joint between the thick coating and substrate.

The parameters of intense ion assistance needed for decreasing the temperature of synthesis of α-Al_2O_3 coatings strongly affect the phase composition, microstructure and level of intrinsic stresses in the coating [1]. The range of substrate temperatures and ion energies, in which the deposition of species from the filtered plasma of the cathode arc forms single-phase α-Al_2O_3 coatings, has been experimentally determined in the paper [2]. When the substrate temperature decreased, the required ion energy increased and amounted to 150 eV at 700°C. However, treatment by ions with energy in the range 100–200 eV range leads to the growth of lattice microstrains and an increase in the level of intrinsic stresses in the coating [3]. Therefore, it seems appropriate to use ions of lower energies for obtaining thick coatings and to provide the necessary level of energy introduced into the growing coating by increasing the ion current density. However, as the deposition rate grows, it is required to increase the density of ion assistance current, and so more research is needed in order to assess the potential implementation of this approach.

Low-temperature formation of α-Al_2O_3 at low rates of coating deposition, low intensity of ion assistance, low gas pressures and an almost stoichiometric ratio of particle flows on the surface of coating provide localized epitaxial growth of α-Al_2O_3 on a sublayer of the material that is used as a crystallographic template, such as Cr_2O_3 [4]. However, highly unbalanced conditions of coating deposition at high densities of the vaporized particle flow and ion current do not allow localized epitaxial growth of α-Al_2O_3 [5]. Studies of the microstructure of Al_2O_3 coatings deposited from the filtered plasma of a cathodic arc with ion assistance at low-temperature have demonstrated that first a homogeneous structure containing an amorphous phase and γ-phase microcrystals is formed on the substrate [2]. Then, the γ-phase initiates the growth of large wedge-shaped crystallites. This growth pattern of the α-phase leads to the heterogeneity of the coating in thickness because α-phase crystallites closeuponly after the coating reaches a certain thickness. However, a number of studies have shown the very rapid formation of the α-phase, usually at highly intensive ion irradiation [6, 7].

The authors [8] have concluded that the recrystallization of the γ-phase with apredominant orientation of the crystal lattice (110) and the subsequent growth of the α-phase with a texture (100) take place during low-temperature deposition of Al_2O_3 coating. Thus, the mechanism of γ-α recrystallization inevitably determines the formation of textured α-Al_2O_3 coatings, the microstructure and properties of which are currently under-researched.

This paper sets out conditions for achieving high-speed growth of coatings with α-Al_2O_3 structure and a low level of intrinsic stresses, providing high adhesion of coatings with a thickness up to 10 μm, synthesized through reactive deposition from plasma in the arc with an evaporated anode at 640°C. The results of the XRD analysis of the phase composition, microstructure, and intrinsic stresses in coatings deposited at low bias voltages (-50 V) are presented. The dependencies of the growth rates of coatings with a stoichiometric composition on the oxygen flow and plasma density have been investigated and explained based on the results of measurements of the plasma composition by optical spectroscopy.

2. Experimental technique

Evaporation of Al and deposition of coatings took place in the discharge plasma with a self-heated hollow cathode, thermo-isolated anode-crucible and water-cooled hollow anode with an aperture area ~ 1 cm^2. A detailed description of the device is provided in the paper [9]. The thermo-isolated crucible was chosen due to the fact that it is heated with a lower density of electron current than a forced cooling crucible, and thus the ionization degree of metal vapor is reduced. This results in a decrease in the proportion of Al ions in the ion flow to the surface of the growing coating accelerated by bias voltage and acceleration of γ-α transformation [5]. An Al portion with a weight of 0.3 g was loaded into a graphite crucible with a diameter of 8 mm. The plasma ionization degree was increased using the heterogeneous magnetic field of a solenoid installed outside the hollow cathode. The hollow cathode and anode-crucible were placed at a distance of 250 mm from each other; the hollow anode and sample holder were installed normally to the axis of the system at a distance of 100 mm from the crucible.

Ar was supplied through a hollow cathode (40 sccm). O_2 was supplied through a hollow anode; its flow rate was regulated in the range of 50–200 sccm. The total discharge current reached 40 A. Part of discharge current (2.5–4 A), which was closed on the anode-crucible, provided heating and evaporation of Al. The current on the hollow anode, which varied between 8 and 36 A, determined the density of the ion current from the plasma and the degree of O_2 dissociation. At the constant current of the magnetic coil, the density of ion current depended linearly on the anode current I_a, as j_i [mA·cm^{-2}] = $k \cdot I_a$ [mA], where $k = 4\times10^{-4}$ cm^{-2}. The pulse bias voltage was supplied to the sample holder (-50 V, 50 kHz, 10 μs).

The coating was deposited to the AISI430 stainless steel substrate with a 0.1–0.2 μm thicksublayer of Cr_2O_3 and without it. The deposition time was 0.5 h; the thickness of the coating varied between 1.5–10 μm depending on the application modes. The vacuum chamber was pumped out by a

turbomolecular pump, residual pressure was 10^{-3} Pa, and the working pressure of the gas mixture Ar+O_2 was 0.1–0.4 Pa.

The temperature of substrates (640°C) was set by a heater and measured by a thermocouple, the readings of which were controlled by an optical method using an Optris CT fast pyrometer, operating in the temperature range of 50–975°C. Control measurements have shown that changes in discharge current and bias voltage in the above working range cause changes in substrate temperatures by maximum 5°C.

The plasma radiation spectrum was recorded using an R2000 fiber optic spectrometer (OceanOptics) operating in the wavelength range of 190–1100 nm. The spectra were registered perpendicular to the discharge axis, at 30 mm away from the crucible. Optical spectroscopy was used to monitor the permanence of the Al evaporation rate during the coatings deposition, as well as to study the effect of the discharge parameters on the discharge plasma composition. The micro-hardness of coatings was determined by the ultramicrohardness tester DUH-211/211S at penetration depth not exceeding 10% of the coating thickness. The thickness of the coatings was measured using a Calotest device; X-ray analysis was carried out using an XRD-7000 diffractometer. The structure of the films in cross-section and on the surface of the coating was studied using an electron microscope LEO 982.

3. Results

Al_2O_3 coatings were deposited on the samples with and without a Cr_2O_3 sublayer at bias voltage U_b = -50 V, substrate temperature of 640°C and various values of discharge current I_a and oxygen flow Q_{O2}. The proportion of the α-phase in 1.5 μm thick coatings determined by the XRD method increased along with I_a and reached ~ 100% at $j_i > 10$ mA·cm^{-2} [5]. The coatings obtained at U_b = -50 V are characterized by lower levels of microdistortion (0.06–0.14%), intrinsic stresses (1.5–2 GPa), larger SCR (45–75 nm) compared to previously obtained coatings at U_b = 100–200 eV in [9].

Experiments have shown that the Al evaporation rate at a constant current in the crucible chain I_c depends on the discharge parameters and the duration of the evaporation cycle, so the intensity of the line Al* (396 nm) of optical emission spectrum of plasma (OES) was controlled during measurement of the growth rate of the coatings. Current I_a affects power incoming to the crucible due to changes in near-electrode potential drops in an arc with a self-heated hollow cathode and hollow anode. The growth of I_a leads to a decrease in the cathode potential drop, an increase in the potential drop in the space charge layer at the entrance to the anodic cavity and a decrease in the positive potential drop in the near-electrode layer at the crucible (figure 1). As a result, both directional and chaotic velocities of electrons entering the anode decrease, the heating power of the crucible decreases, and accordingly, the rate of metal evaporation from the crucible also decreases [5].

Measurements of the coating thickness at a constant intensity of the Al* (396 nm) line have shown that the coating growth rate depends on I_a and Q_{O2} (figure 2). The elemental composition of Al_2O_3 coatings measured at constant evaporation power was approaching the stoichiometric one with an increase in Q_{O2} up to ~ 30 sccm [9]. A further increase in Q_{O2} caused an increase in the coating growth rate. Since at large Q_{O2} through the hollow anode, discharge voltage, crucible heating power, and Al evaporation rate are virtually independent of Q_{O2}, the increase in the deposition rate of coatings may be caused by processes in the plasma or on the surface of the growing coatings that facilitate more efficient use of plasma species during the formation of the coating.

Assessments have shown that in the conditions of the experiment, the mass of Al evaporated during deposition of the coating is several times greater than the theoretical mass of Al in the coating estimated for a hemisphere with aradius of 100 mm according to the Lambert–Knudsen law [10] and Q_{O2} through the anode exceeds the flow of evaporated Al atoms by 2–3 orders of magnitude. Therefore, the probability of reflection of incident species from the surface and desorption of adsorbed species is quite high.

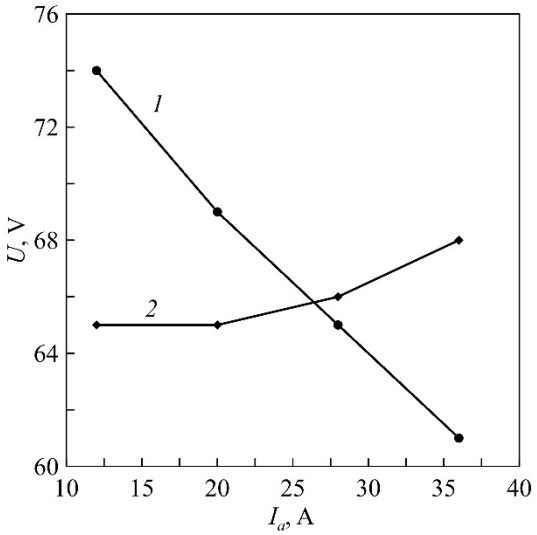

Figure 1. Dependencies of the potential difference between the cathode and crucible (1), the cathode and hollow anode (2) on the hollow anode current.

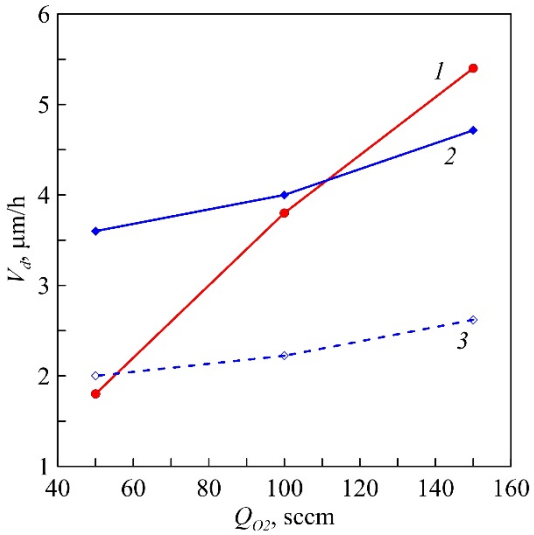

Figure 2. Dependencies of the coating deposition rate on the O_2 flow. Current in the hollow anode circuit: *1* – 36 A; *2*, *3* – 20 A.

The OES was measured at various parameters and conditions of discharge operation. Figure 3 demonstrates the dependencies of line intensities of atomic O*(777 nm) and Al* (396 nm) in the OES on Q_{O2} through the hollow anode. An increase in the line intensity of O indicates a significant increase in the concentration of O in plasma, while the intensity of the Al line in the plasma monotonously decreases with growing Q_{O2}. Figure 4 shows the pattern of changes in the intensity of the O line (777 nm) in the discharge current function, indicating a multiple increase in the O_2 dissociation degree along with the increasing current.

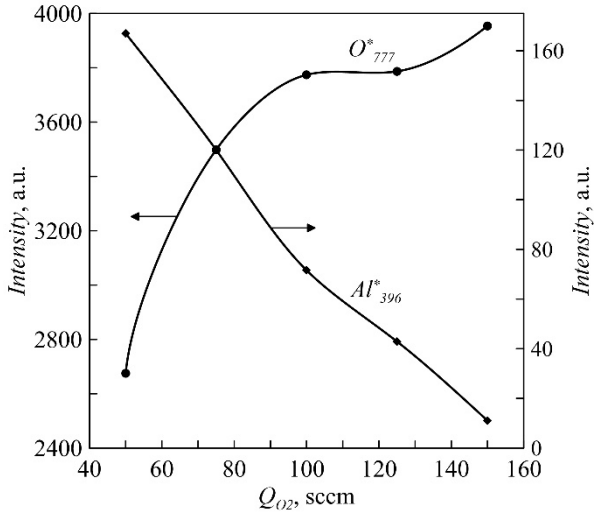

Figure 3. Dependencies of the intensity of lines of atomic O^* and Al^* on the O_2 flow.

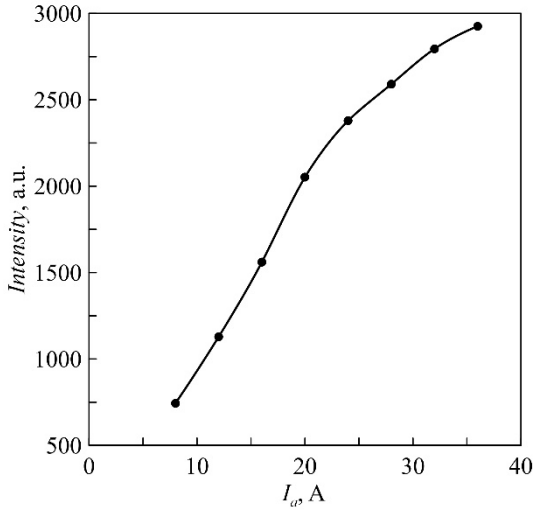

Figure 4. Dependency of the intensity of atomic O^* lines on the current in the hollow anode circuit.

The growth rate of coatings deposited at the same intensity of the Al* line and different values of I_a increases almost linearly with increasing Q_{O2}. The growth rate changes to a lesser extent at lower I_a (figure 2). However, the same intensity of the Al* line at different I_a does not mean that Al evaporation rates are equal, as increasing I_a and the density of the electronic component of plasma results in increased frequency of collisions between electrons and Al atoms and, therefore, the intensity of the Al* line also increases. Consequently, at lower I_a (20 A), the experimental evaporation rate was higher than at I_a = 36 A, which is confirmed by the difference in the average current values I_c: 3.1 A at I_a = 36 A and 3.4 A at I_a = 20 A. If the dependency of plasma density on discharge current is of a linear character, then at equal rates the ratio of intensities of thelines $Al^*_{36\ A}/Al^*_{20\ A}$ should roughly correspond to the ratio of currents (~ 1.8). As a result, at equal Al evaporation rates, the dependency of the deposition rate for I_a = 20 A will be located below dependency obtained at the anode current 36 A (curve 3 in figure 2). Thus, the coating deposition rate increases along with the growth of both Q_{O2} and I_a. At maximum I_a = 36 A, the increase in Q_{O2} from 50 to 150 sccm resulted in a 3-fold increase in the coating deposition rate.

XRD patterns of coatings obtained by high-speed deposition under the conditions of high values of Q_{O2} and I_a are shown in figure 5. The coatings are single-phase (α-Al_2O_3) and have a predominant orientation of the crystal lattice (300). The type of the obtained XRD patterns does not depend on the presence or absence of the Cr_2O_3 sublayer. The average grain size monotonously decreases from 80 to 65 nm with increasing Q_{O2} from 50 to 150 nm, while microdistortions grow from 0.08 to 0.1%. The analysis of the XRD patterns has revealed compressive residual stresses in coatings, the value of which does not exceed – 1.5 GPa. The microhardness of coatings was 22–24 GPa; the Young modulus was 250–278 GPa.

Figure 6 shows an electronic microscopic image of a cross-sectional of the coating with a thickness of 10 μm deposited for 2 h. The coating has a dense homogeneous structure. There are no cracks or detachments at the interfaces “coating – sublayer – substrate”.

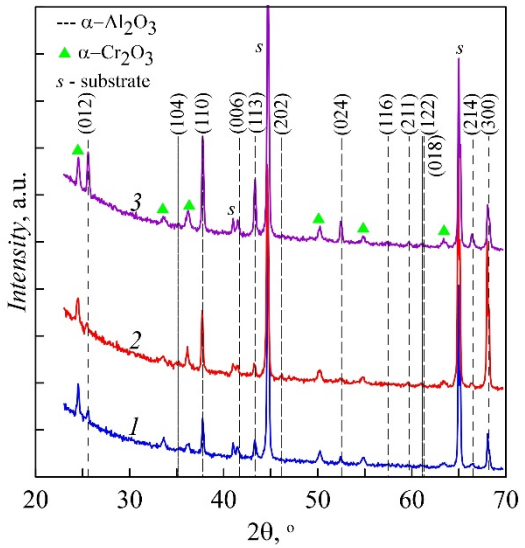

Figure 5. XRD spectra of the Al_2O_3 coatings. O_2 flow rate: *1* – 50 sccm; *2* – 100 sccm; *3* – 150 sccm. Anode current 36 A.

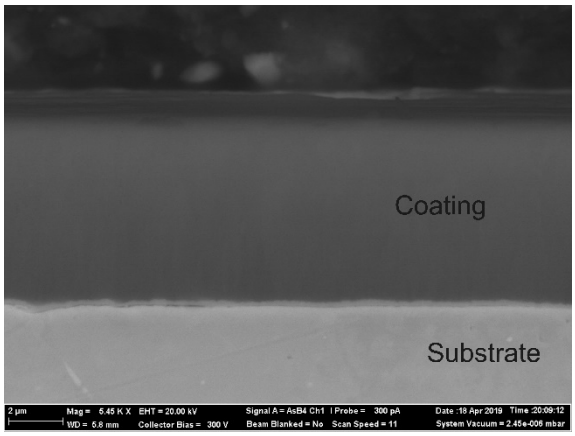

Figure 6. SEM image of the cross-section of Al_2O_3 coating.

4. Discussion

It was concluded in the work on the synthesis of thin Al_2O_3 films using the powerful pulsed magnetron sputtering method that the approach towards achieving low-temperature growth of α-Al_2O_3 coatings is

not just high-energy ion bombardment, but rather bombardment with ions with optimal energy and the use of sufficiently high ion fluxes [11]. This conclusion is consistent with the results of the simulation of the α-Al_2O_3 growth process using the molecular dynamics method, which allows talking about the presence of the ion energy range that is optimal for the formation of α-Al_2O_3 [12].

The results of this work confirm that the combination of low-energy ions (50 eV) and high average ion current density (10–15 mA·cm^{-2}) ensures the formation of low-stressed Al_2O_3 coatings with 100% content of the α-phase, regardless of the presence or absence of the orienting sublayer. In accordance with the conclusions [5] about the significant effect of the ionization degree of metal vapor on the rate of γ-α transformation, the content of Al ions in the ion flow on the growing coating has been minimized.

Formation of α-Al_2O_3 through γ-α recrystallization has been studied in a number of works. This phase transition was observed both under the influence of ion irradiation [8] and during annealing of the amorphous Al_2O_3 coating [13, 14]. Studies of the structure resulting from unfinished γ-α transition during annealing of amorphous Al_2O_3 coating with a thickness of 0.14 μm at 1200°C for 2 h have shown that it consists of large (1 μm) microcrystallites of the α-phase inside the fine-grained γ-phase with the size of nanocrystallites up to 50 nm [14]. Near the grains of the α-phase with a prevailing texture (300), nanocrystals of the γ-phase had a predominant orientation (440), which ensured the correspondence of the crystal lattices of the γ and α-phases. This paper puts forward a hypothesis about the existence of a mechanism of the abnormally rapid growth of the α-phase resulting from interface-controlled phase transformation, in which α-Al_2O_3 is being formed along certain crystallographic planes of the parent γ-phase. A similar conclusion that low-temperature deposition takes place in the process of recrystallization of the γ-phase with a predominant orientation of the crystal lattice (110) and the α-phase with a texture (100) was made in the work [8]. It should be noted that under the conditions of localized epitaxial growth of α-Al_2O_3 on Cr_2O_3, the orientation relationship $[011]_{Al2O3}/[011]_{Cr2O3}$ is implemented [15]. Thus, the presence of (300) texture in the investigated coatings confirms the implementation of the mechanism of γ-α recrystallization in coatings formed under high-speed deposition conditions.

The dependence of the coating growth rate on Q_{O2} and I_a is due to the significant impact of these parameters on the content of atomic oxygen in the plasma. It is known that oxygen dissociation in Ar-O_2 discharge can be caused by the collision of an oxygen molecule with an electron having energy over 4.5 eV [16] or a collision with a metastable Ar atom [17]. Since the concentration of Ar in discharge decreases with the growth of Q_{O2}, the first mechanism is most likely. In addition, the combination of increased oxygen pressure in the anode discharge cavity and the presence of a dense flow of electrons accelerated in the anodic potential drop creates the most favorable conditions for dissociation of oxygen by electron impact. If the growth of Q_{O2} increases the concentration of atomic oxygen, then the growth of I_a increases the degree of oxygen dissociation in the plasma, as well as j_i and energy introduced into the growing film.

Changing the ratio between atoms and molecules in the oxygen flow on the surface of the coating affects the oxygen absorption rate. Dissociation of the oxygen molecule in the plasma requires the energy of 5 eV [18], so the increasing proportion of oxygen atoms in the flow should, in principle, reduce the energy costs of coating formation. In addition, on certain crystallographic planes, absorption of oxygen atoms may be accompanied by the formation of a more stable and strong bond with the lattice than in the case of dissociative absorption of molecular oxygen [7]. More detailed investigation of this complex problem is beyond the scope of this article.

5. Conclusion

High-rate deposition of thick (~ 10 μm) α-Al_2O_3 coatings at 640°C has been performed using the low-energy (-50 V) ion assistance mode with a high density of ion current (up to 15 mA·cm^{-2}), which contributes to the formation of the α-phase with a minimal level of microdistortions (not more than 0.1%) and intrinsic stresses (not more than – 1.5 GPa), which is important for providing high adhesion of the thick coating.

A high coating deposition rate achieved by increasing the oxygen flow and plasma density is due to an increase in the proportion of atomic oxygen in the flow of particles on the coating surface, which excludes energy costs of dissociation of oxygen molecules on the coating surface and changes the dynamics of the oxygen adsorption process.

The absence of significant differences in the phase composition and microstructure of coatings obtained using the crystallographic pattern and without it, as well as the emergence of preferential orientation (300) of the crystal lattice of the α-phase, indicate that the formation of the α-phase occurs through γ-α transformation.

The single-phase adhesion-strong α-Al_2O_3 coatings with a thickness up to 10 μm and a deposition rate up to 5 $m \cdot h^{-1}$ have been obtained. The micro-hardness of the coatings was 22–24 GPa, and the Young modulus was 250–280 GPa.

Acknowledgments
This work was supported by the Russian Science Foundation (grant No. 18-19-00567).

References
[1] Kyrylov O, Kurapov D and Schneider J M 2005 *Appl. Phys. A* **80** 1657
[2] Brill R, Koch F, Mazurelle J, Levchuk D, Balden M, Yamada-Takamura Y, Maier H and Bolt H 2003 *Surf. Coatings Technol*. **174–175** 606
[3] Davis C A 1993 *Thin Solid Films* **226** 30
[4] Jin P, Xu G, Tazawa M, Yoshimura K, Music D, Alami J and Helmersson U 2002 *J. Vac. Sci. Technol. A* **20** 2134
[5] Gavrilov N V, Kamenetskikh A S, Trernikov P V, Emlin D R, Chukin A V and Surkov Yu S 2019 *Surf. Coatings Technol*. **359** 117
[6] Yamada-Takamura Y, Koch F, Maier H and Bolt H 2001 *Surf. Coatings Technol*. **142–144** 260
[7] Wallin E, Selinder T I, Elfwing M and Helmersson U 2008 *EPL* **82** 36002
[8] Zywitzki O and Hoetzsch G 1997 *Surf. Coat. Technol*. **94–95** 303
[9] Gavrilov N V, Kamenetskikh A S, Tretnikov P V and Chukin A V 2018 *Surf. Coatings Technol*. **337** 453
[10] Maissel L I and Glang R 1970 *Handbook of Thin Film Technology* (McGraw Hill Hook Company)
[11] Liu H, Tao J, Xu J, Chen Z and Luo X 2010 *Appl. Surf. Sci.* **256** 5939
[12] Houska J 2013 *Surf. Coatings Technol*. **235** 333
[13] Chou T C and Nieh T G 1992 *Thin Solid Films* **221** 89
[14] Chou T C and Nieh T G 1991 *J. Am. Ceram. Soc*. **74(9)** 2270
[15] Jin P, Nakao S, Wang S X and Wang L M 2003 *Appl. Phys. Lett.* **82(7)** 1024
[16] Gudmundsson J T and Thorsteinsson E G. 2007 *Plasma Sources Sci. Technol.* **16** 399
[17] Bogaerts A 2009 *Spectrochimica Acta Part B* **64** 1266
[18] Andersson J M, Wallin E, Chirita V, Munger E P and Helmersson U 2005 *Phys. Rev. B* **71** 014101